AAPS PharmSciTech, Vol. 14, No. 1, March 2013 (© 2012)
DOI: 10.1208/s12249-012-9900-6

Research Article

The Experimental Evaluation and Molecular Dynamics Simulation of a Heat-Enhanced Transdermal Delivery System

Daniel P. Otto[1] and Melgardt M. de Villiers[2,3]

Received 22 August 2012; accepted 20 November 2012; published online 11 December 2012

Abstract. Transdermal delivery systems are useful in cases where preferred routes such as the oral route are not available. However, low overall extent of delivery is seen due to the permeation barrier posed by the skin. Chemical penetration enhancers and invasive methods that disturb the structural barrier function of the skin can be used to improve transdermal drug delivery. However, for suitable drugs, a fast-releasing transdermal delivery system can be produced by incorporating a heating source into a transdermal patch. In this study, a molecular dynamics simulation showed that heat increased the diffusivity of the drug molecules, resulting in faster release from gels containing ketoprofen, diclofenac sodium, and lidocaine HCl. Simulations were confirmed by *in vitro* drug release studies through lipophilic membranes. These correlations could expand the application of heated transdermal delivery systems for use as fast-release-dosage forms.

KEY WORDS: diffusion; heated patch; ketoprofen; molecular dynamics; transdermal.

INTRODUCTION

The transdermal delivery route is sometimes preferred when the oral route is not feasible, to avoid first-pass metabolism, or for local application of an affected area which often hinders the success of oral drug administration due to poor oral bioavailability as seen for propranolol which shows only 23% oral availability (1–4). However, absorption of drugs or other agents through the skin is slow compared with parenteral routes or the popular oral route (5–7). This is because a significant barrier to drug permeation is posed by the stratum corneum, the outermost layer of the epidermis of the skin, limiting the extent of delivery of xenobiotics through the skin (8).

The barrier function can, however, be compromised to enhance the delivery of agents through the skin. Chemical penetration enhancers associate with the lipid bilayers and compromise the structure of the bilayers to weaken the barrier function (9). Other methods include microneedle arrays (10), electroporation (11), laser ablation (12), and phoresis methods (13,14). In the management of pain, it has often been found that the application of localized heat prior to topical application of therapeutic agents, such as fentanyl (15,16), resulted in a marked improvement in the absorption of the drug. It was suggested that an increase in blood perfusion, due to heating the skin surface, resulted in higher absorption of the drug. Testosterone was also successfully administered transdermally to treat hormone insufficiency, with heat showing a beneficial effect (17). Nitroglycerin absorption through the skin was also improved significantly if heat was applied (18).

In this context, several examples of heated devices have been developed to apply heat to a target are of topical administration to improve drug absorption. An example is the employment of microheaters (19), devices that are interfaced with the transdermal delivery system, that supply heat to the localized target area. Some patches have incorporated a layer of reagents in the patch that could produce heat when activated. These heat-enhanced patches have been successfully applied for drugs, such as corticosteroids (20) and local anesthetics (21). Nuvo Research Inc. (22) has developed a controlled heat-assisted drug delivery (CHADD™) technology that is already approved for use in several products such as Synera® for the heat assisted topical delivery of lidocaine and tetracaine. The CHADD unit contains a heat-generating powder which produces heat when exposed to air. After an initial rise in temperature, the mild heat generated will reach and maintain a controlled temperature range for a predetermined period of time.

Although it might be apparent that heat will increase release, scant information is available on the molecular mechanism by which heat enhances the release of the drug from these dosage forms. Currently, software packages are available, commercial software, such as Materials Studio® (Accelrys Software Inc.) (23) or open source software, such as GROMACS (24) and LAMMPS (25) that enable the simulation of transport phenomena (26–29). In this study, a

Electronic supplementary material The online version of this article (doi:10.1208/s12249-012-9900-6) contains supplementary material, which is available to authorized users.

[1] Catalysis and Synthesis Research Group, Chemical Resource Beneficiation Focus Area, Faculty of Natural Sciences, North-West University, Private Bag X6001, Potchefstroom, South Africa.
[2] School of Pharmacy, University of Wisconsin-Madison, 777 Highland Avenue, Madison, Wisconsin, USA.
[3] To whom correspondence should be addressed. (e-mail: mmdevilliers@pharmacy.wisc.edu)

commonly administered transdermal NSAID, ketoprofen, was selected to prepare a heat-enhanced transdermal patch that contained the drug in an aqueous poloxamer 407 gel (30). Molecular insight into the mechanism by which heat improves ketoprofen release is provided, by using molecular dynamics (MD) simulations (25–29). The MD simulation and *in vitro* release results complement each other and provide evidence of the usefulness of using computational methods in the design and mechanistic evaluation of transdermal drug delivery from gels. The heated patch system reported here was also tested for the enhanced TDD of the NSAID diclofenac sodium and the local anesthetic lidocaine HCl.

MATERIALS AND METHODS

Materials

Ketoprofen was selected as model, transdermal delivery drug and also selected for computational modeling. Other drugs tested were diclofenac sodium and lidocaine hydrochloride. All drugs were USP grade obtained from Sigma Aldrich. Pluronic® F127 (BASF, NJ) was used as carrier matrix for the drug. Iron powder, sodium chloride, sodium thiosulfate, and activated carbon were of reagent grade (Sigma Aldrich, Milwaukee, WI). Germaben® II-E (ISP Inc./Ashland, Wayne, NJ) was used as preserving agent (comprising propylene glycol, diazolidinyl urea, methylparaben, and propylparaben). Eudragit® L 100 poly(methyl acrylate-*co*-methyl methacrylate) was purchased from Evonik Industries. Propylene glycol and isopropanol was obtained from Sigma Aldrich. Aluminum foil, poly(propylene) (PPr) and poly(ethylene) (PE), sheets were purchased from commercial sources. Poly(ethylene glycol) 400 (PEG400) and glycerol was obtained from Sigma Aldrich. Poly(vinyl pyrrolidone) (PVP) was obtained from BASF (NJ).

Patch Construction

Preparation of Gels

Ketoprofen gel was prepared by solubilizing ketoprofen in isopropanol and then adding propylene glycol to this solution. Thirty grams Pluronic® F127 and 2 mL Germaben® II-E was mixed with 100 mL water. The required amount of drug solution was added to the Pluronic® gel to produce a final ketoprofen concentration of 2% (*w*/*w*). After thorough mixing, the gel was left to set in a refrigerator for 1 h. Diclofenac sodium 2% (*w*/*w*, relative to diclofenac) and lidocaine HCl 2% (*w*/*w*, relative to lidocaine) gels were also prepared using the same method and excipients.

Heating Source

The heat patch comprised 25 g of a chemical mixture of iron powder, sodium chloride, sodium thiosulfate, activated carbon, and water that was sealed between the PPr and aluminum foil sheets which both measured 5×2.5 cm. The PPr sheet served as the top-most layer of the patch (Fig. 1) and insulated the top of the patch. The alumina foil served as the heat conducting layer. A small hole of approximately 1 mm diameter was pierced in the PPr sheet and sealed airtight with a suitable adhesive sticker. Care was taken to prevent unnecessary exposure of the chemical mixture to air and the patch was sealed immediately after transfer of the reagents to the sheet reservoir.

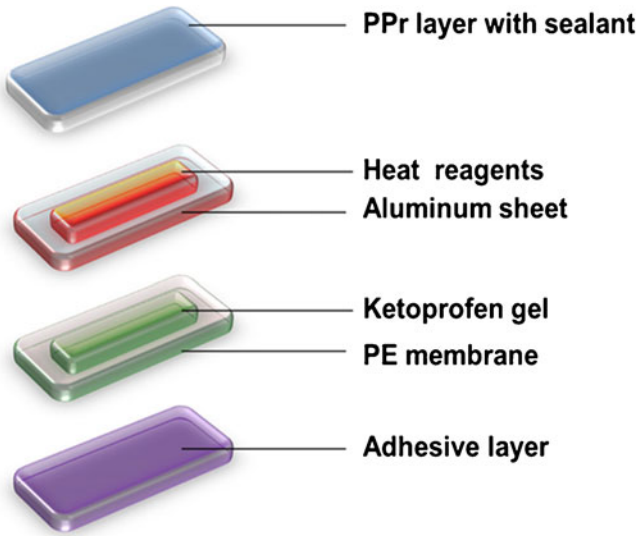

Fig. 1. The various layers incorporated to produce the transdermal patch. Components are not drawn to scale

Permeable Membrane and Adhesive Layer

The requisite quantity of the ketoprofen gel was transferred onto a PE membrane through which the drug could permeate. The gel was evened out over the membrane followed by attachment of the heat patch on top of this layer. Therefore, an even gel layer was formed that directly contacted the aluminum layer for heat conduction.

The Eudragit® was plasticized with PEG400 and glycerol with addition of a further 5% PVP before casting this pressure-sensitive adhesive film. This drug-permeable, pressure-sensitive adhesion film was cut to the correct size and transferred onto the PE membrane containing the drug. This thin adhesive film constituted the bottom-most layer of the patch system. Figure 1 depicts the transdermal patch delivery system.

EXPERIMENTAL

Heating Source Performance

The chemical mixture that was employed for generating heat was mixed in a plastic vial and some vermiculite was added to serve as insulator (not used in patch). Five milliliters of water was added to approximately 25 g of the chemical mixture in the vial, and the vial was capped and shaken for 30 s. A hole of approximately 1 mm diameter was pierced in the lid to mimic that of the PPr layer of the transdermal patch. The heating reaction started after approximately 1 min, and thereafter, temperature was measured at regular intervals at a set height (in the middle of the slurry) in the container.

Release of Drugs from the Gels

An enhancer cell system was used to determine drug release from the 1-g samples of the gels. A Vanderkamp 600 six-station dissolution tester (VanKel Corp., Cary, NC) was employed at temperatures ranging from 32 to 42°C which was adjusted in 2°C increments. The dissolution vessels (200 mL flat bottom) were filled with 200 mL deionized water as dissolution medium and the gel-loaded enhancer cells rotated in the medium at 50 rpm. Samples were withdrawn at regular intervals spanning the duration of 1 h, filtered and analyzed by HPLC. After sampling, the vessels were replenished with deionized water equal to the sampling volume. Samples were analyzed for drug content using HPLC methods published in the USP for chromatographic purity of ketoprofen and diclofenac sodium, and the content analysis of lidocaine HCl topical solution.

Diffusion Studies

Franz-type diffusion cells (12 mL, 15 mm diameter orifice, Permagear Inc., Hellertown, PA) were used to conduct diffusion studies using a cellulose acetate membrane (0.45 μm pore diameter). The cellulose acetate membrane was soaked in 15% (*v*/*v*) oleic acid in isopropyl myristate. The receiving chamber of the Franz-type cell was filled with 12 mL deionized water and a magnetic stirrer bar, followed by clamping the membrane between the donor and receiver chambers. The donor chamber was filled with 1 g of the gels. Patches containing the gels were also evaluated by using a modified Franz-type cell that could clamp the patch securely to the membrane. The Franz-type cells were water-jacketed to ensure a temperature of 32°C. One-milliliter samples were withdrawn at 5-min intervals from the acceptor side and replenished with deionized water. The drug content was determined by HPLC. Figure 2 shows the experimental setup for the diffusion studies.

Since release studies were done using lipophilic cellulose acetate membranes the change in skin conductance of volunteers was also measured as a function of time and temperature as a measure of the effect of temperature on skin. For this study, an unmedicated patch was applied to the skin of three volunteers, and the change skin conductance measured as a function of an increase in skin temperature (NeXus Skin Conductance Sensor, Stens Corporation, San Rafael, CA). This instrument uses a two-electrode potential meter. The electrodes were placed at either side of the membrane in the donor or acceptor sides, and the potential was measured. This was converted to conductivity.

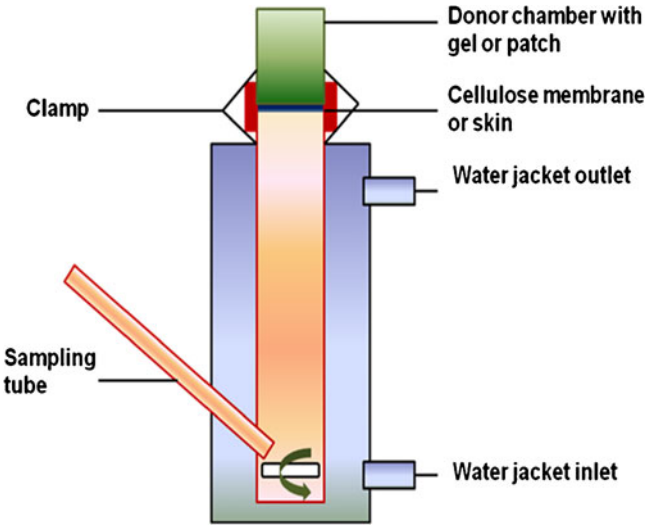

Fig. 2. The experimental setup for the Franz-type diffusion cells

MD Simulation Theory

MD simulation studies consider that Newton's second law of motion (Eq. 1) is solved for each atom at each time step in the simulation.

$$F_i(t) = m_i a_i(t) \tag{1}$$

Where F_i is the total force that a particle, i, with a mass of m_i and an acceleration of a_i experiences. Solving the equation for each atom at each time point (t) in the simulation provides information on its displacement over time, density of the system and other properties such as energetics. In the system here, approximately 6,600 atoms are present in the gel structure for which Eq. 1 is solved, employing the velocity Verlet algorithm for integration (31).

A force field, COMPASS (32) in this case, provides the parameters by which the total forces that act on each atom are computed. This information for instance instructs the calculation of Van der Waals and Coulomb forces within a certain radius of a target atom. At certain interatomic distances set by the user, the correct force can be computed or negated by the switch function defined by these interatomic distance cut-off values. The force field also compiles a list of neighbors for each atom on which forces may act. This list is updated at each time step to determine whether the interatomic distance has changed such that a certain force calculation is still relevant or not. In this way, the correct type of forces can be calculated at each time step for each atom. COMPASS has been extensively validated for condensed matter including polymers, organic and inorganic compounds (32–34).

The forces that evolve in the system can be expressed as a conversion of potential energy to kinetic energy (32). Equation 2 shows a simplified description of the energy expression which results in the atoms experiencing forces that result in their acceleration:

$$E_{\text{total}} = E_{\text{valence}} + E_{\text{crossterm}} + E_{\text{non-bond}} \tag{2}$$

Where E_{valence} represents the energy required for bond stretching, torsion, bending, out-of-plane interactions and configurational interactions. $E_{\text{crossterm}}$ is the energies that lead to distortions or coupling of valence terms. $E_{\text{non-bond}}$ accounts for Coulomb, Van der Waals and hydrogen bonding forces (32).

Ultimately, the position of each atom can be determined at each time step by solving the second law of motion (Eq. 1). This calculation is very complex and no analytical solution exists. Therefore a numerical approximation is performed at each time step in the simulation to solve the matrix of calculations by integration of Eq. 1 using the well-known velocity Verlet algorithm (31) giving a number of three-dimensional positional outputs at each time step for each atom. This results in the calculation of a time-dependent positional trajectory

and the time-dependent displacement of each atom is therefore determined.

MD Simulation

The purpose of the MD simulation was to gain molecular-level insight into the effect of heat on drug release from the gel delivery system. A simplified gel system was used to simulate the gel formulation. Only ketoprofen, water, and Pluronic® F127 were used to construct the model of the gel system. Materials Studio® 6.0 (Accelrys Software Inc., San Diego, CA) was used for all simulations. An HP Compaq® PC, with i5 Intel® core CPUs running at 2.67 GHz and 4 GB RAM, was employed for computations.

Individual Structure Construction and Optimization

Pluronic® F127 (poloxamer 407) was constructed with the Build Polymers tool to comprise a hydrophobic backbone of 56 propylene oxide units flanked on both sides by 101 ethylene oxide blocks (35) with random chain torsion. Structures for ketoprofen and water were constructed in a similar fashion. Figure 3 shows the structures of ketoprofen and poloxamer 407. 10,000 steps were used for energy minimization using the steepest descent algorithm to perform an initial energy minimization preceding the packing of the structures into a periodic box.

Construction of the Gel Structure

The weight fractions of the components in the gel were used to determine the composition of the cell used to represent the gel. The gel comprised 2% ketoprofen, 30% Pluronic® F127, and 68% water based on weight. These were converted to mole fractions and finally, 1 molecule Pluronic® F127, 3 molecules of ketoprofen, and 1,529 molecules of water were included in the cell which was constructed with the amorphous cell module using the construction (legacy) tool with selection of the COMPASS (32) force field option. Nonbonding interactions are computed at a cutoff of 1 nm for the neighbors list. Van der Waals and Coulomb interactions are also computed between 0.85 and 0.95 nm with a switch function to calculate the forces at the cut-off distances. The Coulomb forces were calculated with the Ewald summation method (36). Table I lists the equilibration protocol.

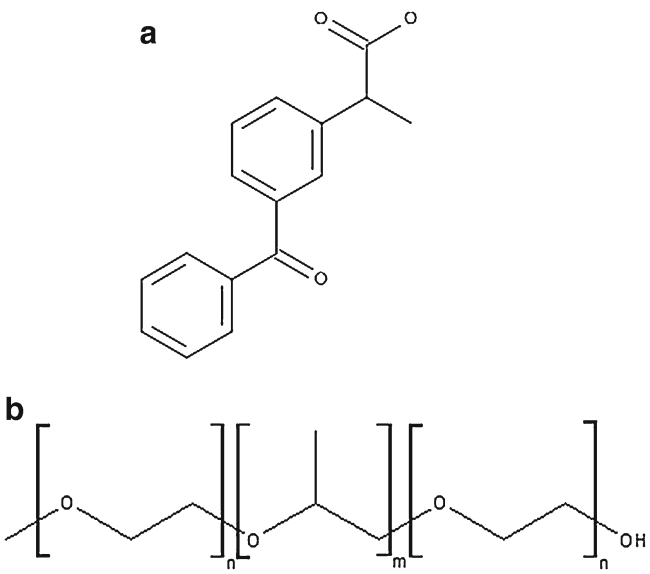

Fig. 3. Structures of **a** ketoprofen and **b** poloxamer 407 (n=101; m=56)

The simulated cell parameters a, b, and c were set at an initial value of 40.63 Å. The targeted density was selected as 1 g/cm^3 since Pluronic® F127 has a density of 1.05 g/cm^3 (39) and water a density of 1 g/cm^3 and make up the bulk of the gel.

The initial geometric structures of the gel were then relaxed using the Discover module in Materials Studio to assume the targeted density. A series of MD procedures were followed to obtain redistribution of the components within the boundaries of the cell. A sequence of constant number of particles, constant volume, and constant temperature (NVT) ensemble constraints were used initially, followed by a sequence of constant particle number, constant pressure, and constant temperature simulations (27,40,41). In this study, an additional equilibration step was added (simulation run 10) to equilibrate the gel at the release temperature preceding the production runs of the dynamics study. During this last step, the density of the cell remained at a constant value of ~1.03 g/cm^3 (see the Electronic Supplementary Material (ESM)).

Diffusivity Calculated by MD

The calculation of the diffusivity of the selected components was performed after the equilibration runs were completed. Production runs were subsequently produced to measure the diffusivity of the selected components. The production runs were conducted on the equilibrated cell in NVT with 5,000 ps dynamics times, at 1 fs step times and with frame output at every 2 ps to produce 2,500 frames and repeated two times for a total of three production runs at each temperature (305 K and 315 K). The mean square displacements (MSD) for the components were determined for each production run, using the Forcite module, and averaged.

To perform the calculations, the water and ketoprofen molecules had to be distinguished from one another as well as from the polymer. This distinction was made on the force field type that the Discover module could interpret according to the COMPASS parameter set. For water, the hydrogen atoms were selected since this force field type occurred only in water and was subsequently encoded according to the COMPASS parameter set as, "h1o". For ketoprofen, the charged carbonyl group was selected and encoded as "o1–". These groups were used as trajectory tracers and their displacement determined by the Forcite module over the 2,500 collected frames created by the Discover dynamics simulation. Figure 4 shows an excerpt of the progression of diffusion from the trajectory file created from one of the dynamics runs.

The increase in temperature experienced by the gel in the patch, due to the heating element of the patch, should result in an increase in Brownian motion of the molecules in the cell. The measure of this motion is known as diffusivity and described by the Eq. 3 (42):

$$D = \lim_{t\to\infty} \frac{\left\langle [r(t) - r(t_0)]^2 \right\rangle}{6t} \tag{3}$$

Where r(t) is the observed displacement of the particle at time t and $r(t_0)$ its original reference position at time t_0. The

Table I. The MD Equilibration Protocol Followed for the 2% Ketoprofen Gel (28)

Simulation run	Ensemble	Simulation time (ps)	Step time (fs)	Temperature (K)
1	NVT	0.2	0.1	300
2	NVT	2	1	600
3	NVT	100	1	300
4	NPT[a]	60	1	300
5	NVT	20	1	750
6	NVT	20	1	600
7	NVT	20	1	450
8	NVT	100	1	300
9	NPT[a]	100	1	300
10	NPT	400	1	Variable[b]

NVT constant number of particles, constant volume, and constant temperature, *NPT* constant particle number, constant pressure, and constant temperature

[a] Pressure was not adjusted in run 4, however was adjusted to 0.1 GPa (1 atm) in run 9 and 10. Pressure was controlled by the Berendsen algorithm (37)

[b] The temperature was adjusted according to the release study conditions. Temperature was controlled by the Andersen algorithm (38)

MSD is given by the squared difference of the two values. D is the diffusivity and is equal to the macroscopic Fickian diffusion constant of numerous particles that experience Brownian movement, therefore the ensemble average MSD of the simulation, $\langle [r(t)-r(t)_0]^2 \rangle$ evolving over time, should equal or reflect the experimental observation according to the ergodic hypothesis.

Therefore the diffusivity for the constituent molecules in the gel was calculated at different temperatures from the particle trajectories (Fig. 4) to determine if temperature influenced the diffusion of the drug molecules from the patch.

RESULTS

Heating Source

The chemical reaction that was exploited here involved the oxidation of the iron powder in the heating source segment of the patch as it is exposed to oxygen. The reaction that takes place is given below (Eq. 4):

$$3Fe + 2O_2 \rightarrow Fe_3O_4 + \text{heat} \tag{4}$$

The heating source showed good performance as determined by the temperature-time profile. Within the first 15 min

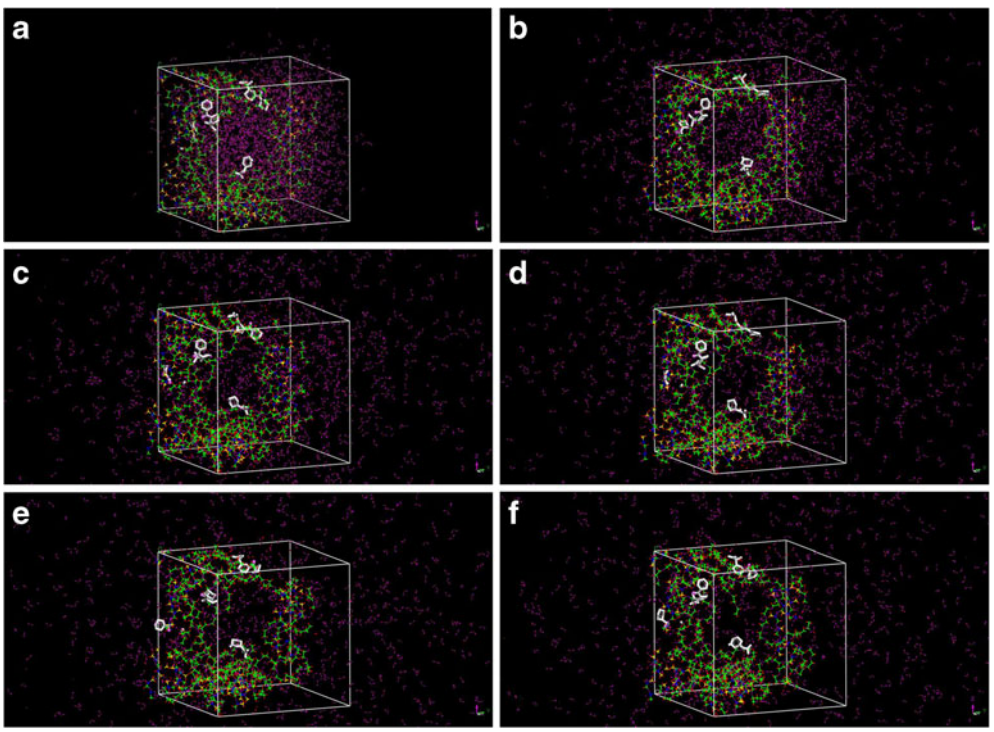

Fig. 4. An excerpt of the trajectory output of the particles in the gel in 833 ps steps (for illustration) at **a** 833, **b** 1,666, **c** 2,499, **d** 3,332, **e** 4,165, and **f** 4,998 ps. Water molecules are shown as *small purple dots*, ketoprofen molecules are shown in *white* (size exaggerated to enhance visibility), and the polymer subunits are shown as long chain structures (*green* and *blue*)

a temperature of ~40°C was reached and the temperature only declined below 37°C after 3 h (Fig. 5). When the reaction mixture was included in the prototype patch it lead to an increase in skin temperature as shown in Fig. 6. Heating the skin also resulted in an increase in skin conductance readings (Fig. 6). The results in Figs. 5 and 6 also showed that the maximum temperature also did not exceed the tolerable value of approximately 40°C, above which patient compliance could become problematic.

Release Studies

Gel

The release of ketoprofen from the gel was monitored at various temperatures as seen in Fig. 7. The drug flux increased linearly from $3.2\times10^3\,\mu g cm^{-2}h^{-1}$ at 32°C to $4.5\times10^3\,\mu g cm^{-2}h^{-1}$ at 42°C (R^2=0.998, n=6, Fig. 7). This represented a 1.4-fold increase in flux when the temperature was raised from 32°C to 42°C. Similarly the drug flux from the diclofenac gel increased 1.7-fold and from the lidocaine gel 1.5-fold. From the results shown in Fig. 7, the beneficial effect of heat on the release rate at an optimal, tolerable temperature of 40°C was clear.

Heated Patch

The drug release from the patch was performed using a modified donor chamber of a Franz-type cell. The orifice of the donor chamber was 15 mm and cellulose acetate membrane soak in a mixture of oleic acid in isopropyl myristate was used (43). As predicted by the gel release studies, the heated patch also performed significantly better than the gel alone (Fig. 8). The drug flux increased from $14.75\pm1.8\,\mu g cm^{-2}h^{-1}$ from the gel to $46.24\pm1.6\,\mu g cm^{-2}h^{-1}$ from the heated patch (Fig. 8). Similarly, the drug flux from the diclofenac gel increased from 13.56 ± 1.8 to $34.86\pm1.7\,\mu g cm^{-2}h^{-1}$ and for the lidocaine gel from 17.99 ± 1.3 to $53.03\pm1.9\,\mu g cm^{-2}h^{-1}$. This represented an increase in flux of around 2.5- to 3-fold for the heated patches.

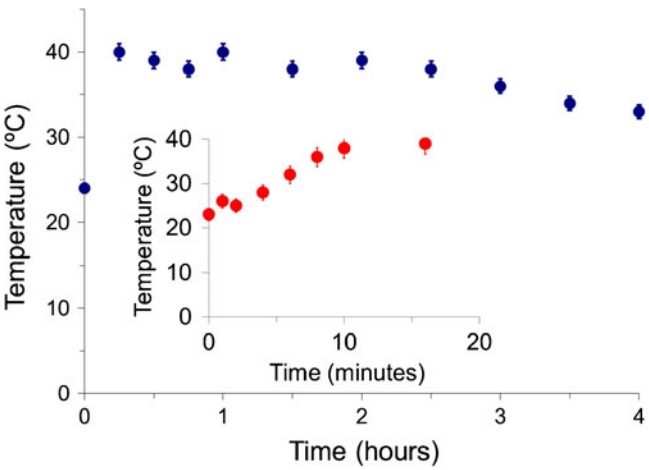

Fig. 5. The temperature *versus* heat profile as measured from the plastic container that was filled with the reaction mixture. The *inset* shows the first 15 min of the reaction

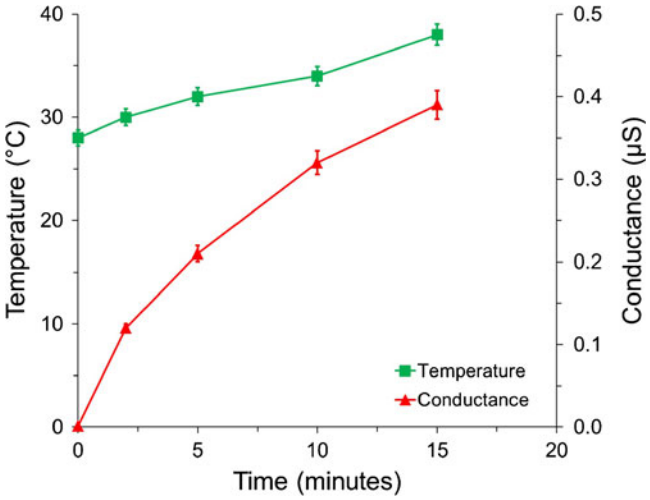

Fig. 6. The effect of heat generated by the patch on the temperature and conductance of the forearm skin of volunteers (n=3)

MD Simulations

Run 10 was the final step in the MD simulation to ensure equilibrium in the system. During equilibration run 9 (Table I), a pressure of 0.1 GPa was applied to approximate atmospheric pressure. It was decided not to adjust pressure during step 4 to allow for more freedom of movement of the components during the relaxation phase. The average density in run 10 that was computed over the simulation time was constant at ~1.026 g/cm^3 which closely approached the target average of 1 g/cm^3 and represents a value between the densities water and Pluronic® F127, the main gel constituents. From the energy profiles it was also confirmed that the system reached equilibrium. It was therefore concluded that the redistribution (steps 1–4), annealing phase (steps 5–9), and temperature equilibration steps were successfully completed (see energy profiles and density profile in the ESM).

To determine if the water and ketoprofen molecules reached the free diffusion state, log(MSD) was plotted *versus* log(t) (Eq. 3). The slope from the regression line should approach unity for free diffusion (27). Examples of the MSD trajectories for water and ketoprofen are shown in Fig. 9a–d, respectively. The diffusion coefficient of water at 32°C was $2.01\times10^{-5}cm^2/s$ and at 42°C $2.39\times10^{-5}cm^2/s$ for a 19% increase, and these values closely approached the experimentally determined values (44) which therefore validated the MD simulation performed here. Ketoprofen demonstrated a D of $1.04\times10^{-7}cm^2s^{-1}$ at 32°C and $1.70\times10^{-7}cm^2s^{-1}$ at 42°C for a 64% increase. This could help to explain the 1.4-fold increase in the release of ketoprofen from the gel when the temperature of the dissolution medium was increased from 32°C to 42°C and the 3-fold increase in the release of the drug from the heated patch.

DISCUSSION

The heating of a localized area on the skin surface could clearly enhance the transdermal absorption of ketoprofen sodium, diclofenac sodium, and lidocaine hydrochloride. This

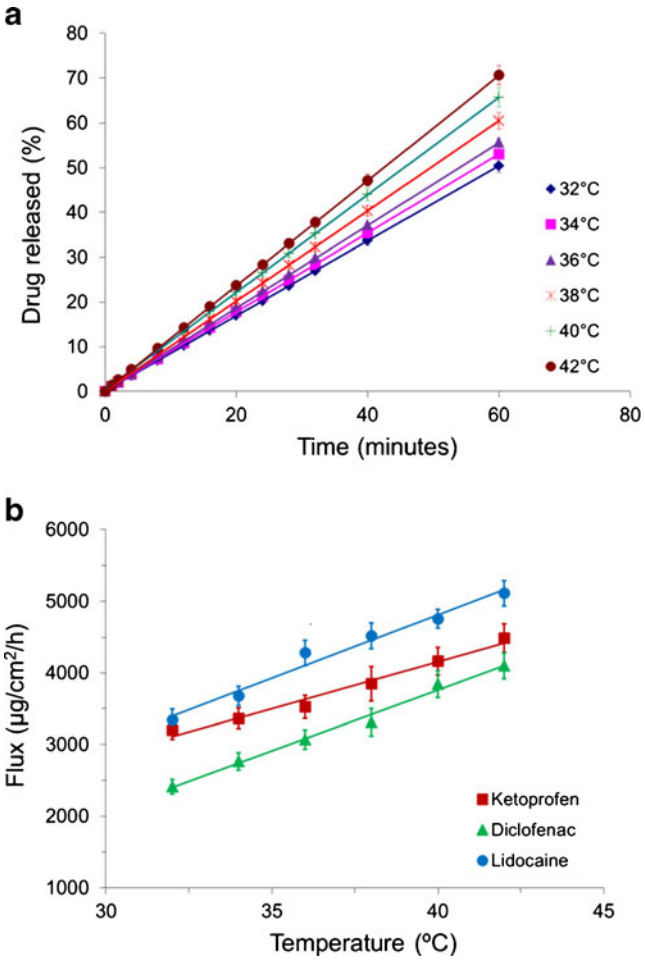

Fig. 7. **a** The release profiles of ketoprofen from the Pluronic® F127 gel in the enhancer system as a function of temperature of the dissolution medium (n=6). **b** Increase in the drug flux from the gels with an increase in the temperature of the dissolution medium (n=6)

effect was best seen at a physiologically tolerable temperature of 40°C. Additionally, at this temperature, changes in skin conductance were also illustrated. This demonstrated an additional advantage of heating since the absorption of the drugs, which are predominantly carried in water as weak electrolytes, could be enhanced compared with the unheated state. Hydration of the skin by water (9) molecules, which are capable of ion conduction, is the most probable mechanism by which drug permeation is enhanced (19). The efficiency of the heating system was also illustrated by the heat profile of the patch system which was maintained within the release period at the desired temperature.

To gain deeper insight into the transport mechanism of the drug release, ketoprofen was employed to simulate drug diffusion based on the classical deterministic Newtonian laws of motion. The evaluation of the simulation results revealed that ketoprofen reached the free diffusive region at a significantly latter stage than water did. Therefore, the first 1,000 ps of the production run were not used for both water and ketoprofen. After this time point, the double-logarithmic plot for ketoprofen approached a slope of ~0.9 which indicated that D could be determined reliably (27,28).

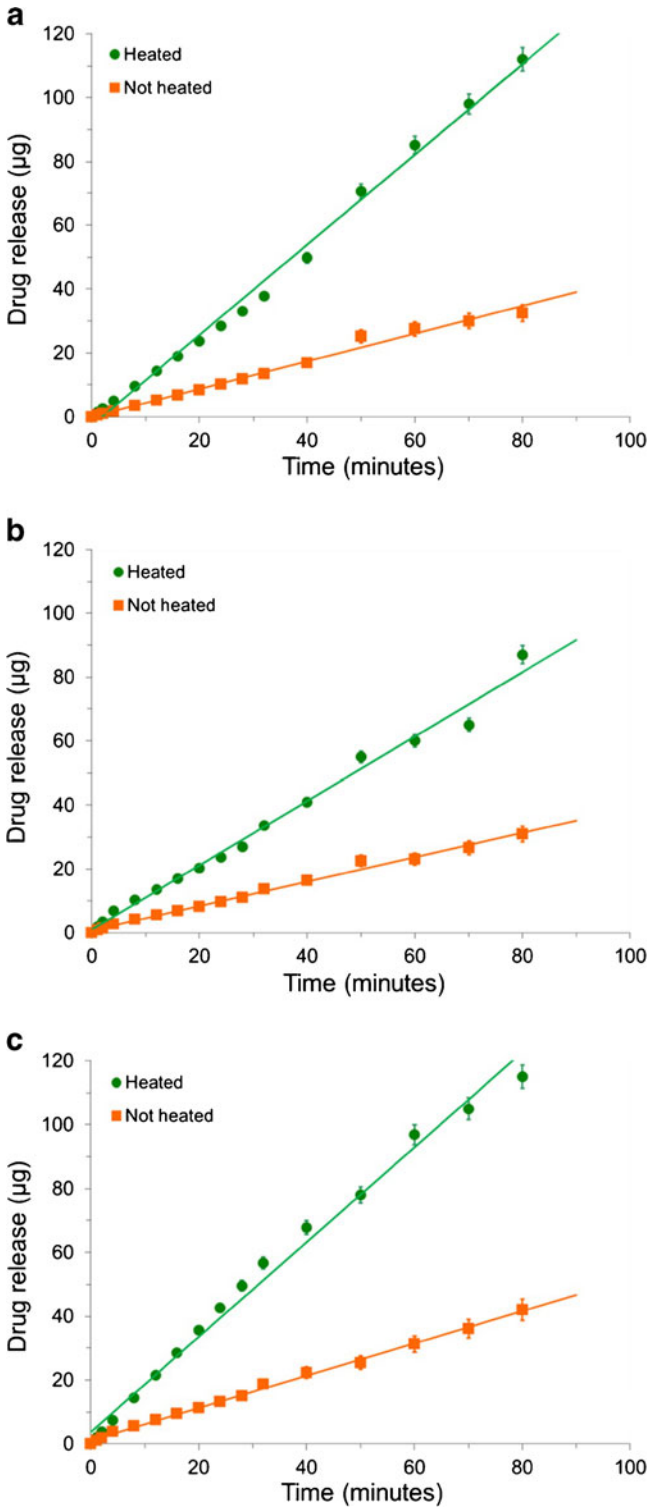

Fig. 8. The release profiles of **a** ketoprofen, **b** diclofenac, and **c** lidocaine from the patch without the heating reagents (*orange symbols*) and the patch containing the heating element (*green symbols*)

Higher values occur during ballistic diffusion (initial phase) and nearing the end of the simulation which are related to initial tension and jump events to in the simulation system (artefacts which are removed by the relaxation and annealing of heterogeneous regions created during the gel construction).

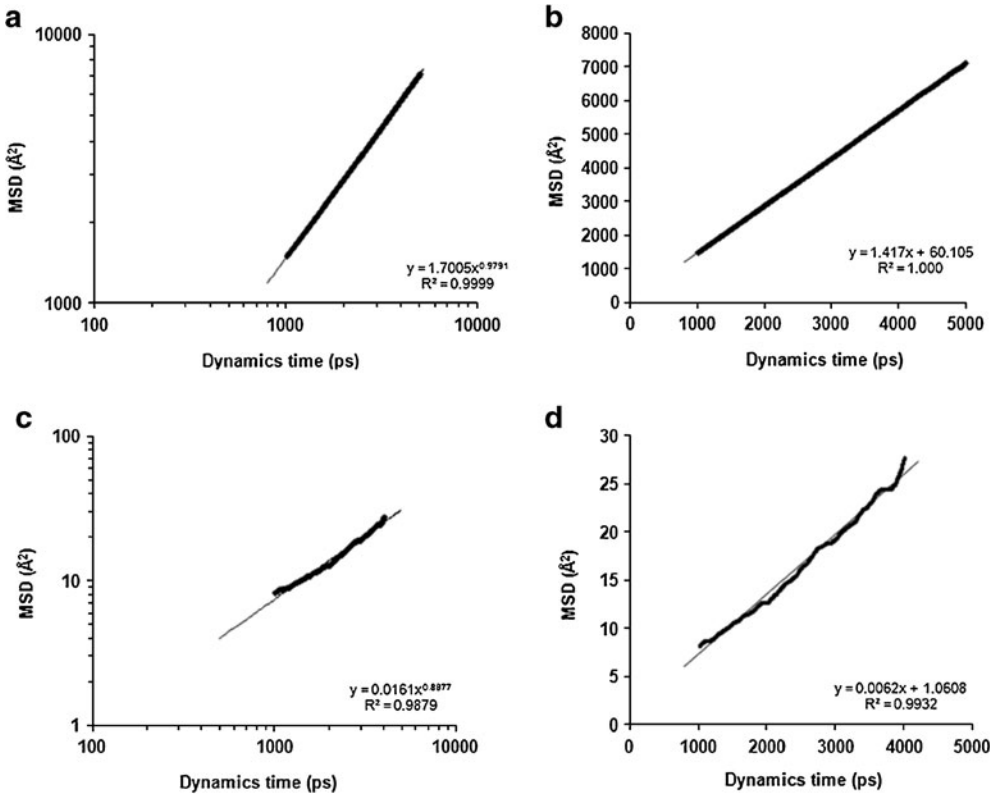

Fig. 9. **a** The double-logarithmic plot of *MSD versus t* for water at 315 K. The exponent of the regression equation is nearly unity; therefore the free diffusion regime is reached. **b** shows the linear increase in MSD *versus t* for the data region selected according to the double-logarithmic plot. The slope of (**b**) is determined and used to calculate the diffusion coefficient (Eq. 3). **c**, **d** Similar evaluations for ketoprofen at 315 K

Lower values indicate that intra- and intermolecular interactions limit the freedom of movement of molecules and therefore the free diffusion of molecules are prevented. Consequently, the linear segment showing a slope of nearly unity, when plotting the double-logarithmic values, is used for calculation of *D* (Fig. 9; ESM). The computer simulation provided a method to study the diffusion mechanism of the drug molecules as well as that of water under the influence of temperature as a variable. The values obtained for the diffusion of water closely resembled the experimentally determined values and therefore validated our simulation models to study ketoprofen. Based on the theoretical knowledge gained for ketoprofen with its experimental confirmation we apply the mechanistic nature of the diffusion process to lidocaine and diclofenac diffusion as well.

The diffusion coefficients increased for both water and ketoprofen as a consequence of an increase in temperature by 10°C. This is not totally unexpected if seen from the Arrhenius relationship between kinetics and temperature (45), although doubling of the coefficients were not seen as is commonly seen for reactions showing typical Arrhenius type behavior. Nonetheless, it is clear that ketoprofen demonstrated higher diffusivity at the higher temperature and therefore explains the increase in release as temperature increases. The change in water diffusivity is a modest 20% and this is attributed to the fact that water is a smaller molecule than ketoprofen and the movement of water molecules is more probable than for ketoprofen. Additionally water enters the free diffusive region at a much earlier stage that for instance ketoprofen and its diffusion coefficient will show a more significant change is the temperature increase was more than 10°C.

Few reports have focused on the very fundamental effect that heat will have on diffusion kinetics (19). Diffusion plays a significant role in drug delivery since the drug needs to diffuse before it can even reach the skin or site of delivery. Additionally, the increase in water diffusion could explain the increase in skin conductance as function temperature. Although temperature increase could damage the skin structure, the experimental temperature did not exceed 42°C. It is doubtful if the skin was structurally damaged to a significant degree by heating.

The increase in the mobility of the drug molecules was reflected in the dissolution and diffusion studies for ketoprofen, diclofenac and lidocaine gels that were evaluated here. From our results, we propose that the heating source had a profound effect on drug diffusion and therefore ultimately on dosage form performance. It is a significant phenomenon that an increase of 10°C experienced by the delivery system could have an effect to change an unheated patch delivery system from a prolonged, sustained release device, to a device of which the release profile resembles some immediate release medications that are administered through other routes.

The heating source that was added to the transdermal patch provides a simple and effective means to enhance drug release. A high rate of release could be achieved with complete release in less than 90 min. This implies the possibility of

using transdermal delivery systems to release drugs at significant rates and to potentially reach significant systemic concentrations when required.

CONCLUSIONS

Molecular insight into the effect of heat on transdermal patch performance points to an increase in diffusivity of the drug and water molecules in the patch. The results obtained the molecular simulation presented here can also aid the theoretical interpretation of experimental results from the very beginning of experimentation. In this instance, we saw that the theoretical basis for diffusion should be enhanced by heat and these assumptions were in fact reflected by the experimental results.

By its maintenance of the desired temperature during the complete release period, the heating system also illustrated the practical efficiency of an economically feasible heat source to produce the desired effect on the transdermal delivery system. It can be suggested that these types of noninvasive dosage forms, with proper theoretical design and experimental evaluation, will make transdermal dosage form design more efficient and eventually result in the desired therapeutic effect and patient compliance which is not always achievable with other routes of administration. Indeed one could potentially create an effective transdermal system which could equal the dose and extent of delivery as seen for oral and parenteral routes.

REFERENCES

1. Pergolizzi JV, Philip BK, Leslie JB, Taylor R, Raffa RB. Perspectives on transdermal scopolamine for the treatment of postoperative nausea and vomiting. J Clin Anesth. 2012;24:334–45.
2. Rao PR, Reddy MN, Ramakrishna S, Diwan PV. Comparative *in vivo* evaluation of propranolol hydrochloride after oral and transdermal administration in rabbits. Eur J Pharm Biopharm. 2003;56:81–5.
3. Walters KA, Brain KR, Green DM, James VJ, Watkinson AC, Sands RH. Comparison of the transdermal delivery of estradiol from two gel formulations. Maturitas. 1998;29:189–95.
4. Xi H, Yang Y, Zhao D, Fang L, Sun L, Mu L, Lu J, Zhao N, Zhao Y, Zheng N, He Z. Transdermal patches for the site-specific delivery of anastrozole. *In vitro* and local tissue disposition evaluation. Int J Pharm. 2010;391:73–8.
5. Muktadir A, Barbar A, Cutie AJ, Plakogiannis FM. Medicament release from ointment bases. III. Ibuprofen: *in vitro* release and *in-vivo* absorption in rabbits. Drug Dev Ind Pharm. 1986;12:2521–40.
6. Sammeta SM, Vaka SRK, Murthy SN. Transcutaneous electroporation mediated delivery of doxepin-HPCD complex: a sustained release approach for treatment of postherpetic neuralgia. J Control Release. 2010;142:361–7.
7. Ammar HO, Ghorab M, El-Nahhas SA, Kamel R. Design of a transdermal delivery system for aspirin as an antithrombotic drug. Int J Pharm. 2006;327:81–8.
8. Bouwstra JA, Honeywell-Nguyen PL. Skin structure and mode of action of vesicles. Adv Drug Deliv Rev. 2002;1(Supple 1):41–55.
9. Williams AC, Barry BW. Penetration enhancers. Adv Drug Deliv Rev. 2004;56:603–18.
10. Sullivan SP, Murthy N, Prausnitz MR. Minimally invasive protein delivery with rapidly dissolving polymer microneedles. Adv Mater. 2010;22:739–43.
11. Prausnitz MR, Bose VG, Langer R, Weaver JC. Electroporation of mammalian skin: a mechanism to enhance transdermal drug delivery. Proc Natl Acad Sci USA. 1993;90:10504–8.
12. Lee WR, Shen SC, Wang KH, Hu CH, Fang JY. The effect of laser treatment on skin to enhance and control transdermal delivery of 5-fluorouracil. J Pharm Sci. 2002;91:1613–26.
13. Kalia YN, Naik A, Garrison J, Guy RH. Iontophoretic drug delivery. Adv Drug Deliv Rev. 2004;56:619–58.
14. Mitragotri S, Blankschtein D, Langer R. Ultrasound-mediated transdermal protein delivery. Science. 1995;269:850–3.
15. Ashburn MA, Ogden LL, Zhang G, Love G, Basta SV. The pharmacokinetics of transdermal fentanyl delivered with and without controlled heat. J Pain. 2003;4:291–7.
16. Carter KA. Heat-associated increase in transdermal fentanyl absorption. Am J Health Syst Pharm. 2003;60:191–2.
17. Shomaker TS, Zhang J, Ashburn MA. A pilot study assessing the impact of heat on the transdermal delivery of testosterone. J Clin Pharmacol. 2001;41:677–82.
18. Klemsdal TO, Gjesdal K, Bredesen JE. Heating and cooling of the nitroglycerin patch application area modify the plasma level of nitroglycerin. Eur J Clin Pharmacol. 1992;43:625–8.
19. Yun J, Lee DH, Im JS, Kim HI. Improvement in transdermal drug delivery by graphite oxide/temperature-responsive hydrogel composites with micro heater. J Mater Sci C. 2012;32:1564–70.
20. Kim KS, Simon L. Modeling and design of transdermal drug delivery patches containing an external heating device. Comput Chem Eng. 2011;35:1152–63.
21. Wood DG, Brown MC, Jones SA. Controlling barrier penetration *via* exothermic iron oxidation. Int J Pharm. 2011;404:42–8.
22. Nuvo Research Inc. (2012) Controlled heat-assisted drug delivery (CHADD™) technology. http://www.nuvoresearch.com/research/chadd.htm. Accessed 16 August 2012.
23. Accelrys Software Inc. Materials Studio® 6.0 (2012) Accelrys Software Inc. San Diego, USA. http://www.accelrys.com. Accessed 04 June 2012.
24. Hess B, Kutzner C, Van der Spoel D, Lindahl E. GROMACS 4: algorithms for highly efficient, load-balanced, and scalable molecular simulation. J Chem Theory Comput. 2008;4:435–47.
25. Plimpton S. Fast parallel algorithms for short-range molecular dynamics. J Comput Phys. 1995;117:1–19.
26. Chaharati SG, Stern SA. Diffusion of gases in silicone polymers: molecular dynamics simulations. Macromolecules. 1998;31:5529–38.
27. Hofmann D, Fritz L, Ulbrich J, Schepers C, Boehning M. Detailed-atomistic molecular modeling of small molecule diffusion and solution processes in polymeric membrane materials. Macromol Theor Simul. 2000;9:293–327.
28. Gautieri A, Mezzanzanica A, Motta A, Redealli A, Vesentini S. Atomistic modeling of water diffusion in hydrolytic biomaterials. J Mol Model. 2012;18:1495–502.
29. Gautieri A, Vesentini S, Redaelli A. How to predict diffusion of medium-sized molecules in polymer matrices. From atomistic to coarse grain simulations. J Mol Model. 2010;16:1845–51.
30. Dumortier G, Grossiord JL, Agnely F, Chaumeil JC. A review of poloxamer 407 pharmaceutical and pharmacological characteristics. Pharm Res. 2006;23:2709–28.
31. Verlet L. Computer experiments on classical fluids. I. Thermodynamical properties of Lennard-Jones molecules. Phys Rev. 1967;159:98–103.
32. Sun H. COMPASS: An *ab initio* force-field optimized for condensed-phase applications—overview with details on alkane and benzene compounds. J Phys Chem B. 1998;102:7338–64.
33. Sun H, Rigby D. Polysiloxanes: *ab initio* forcefield and structural, conformational and thermophysical properties. Spectrochim Acta A. 1997;53:1301–23.
34. Spyriouni T, Vergelati C. A molecular modeling study of binary blend compatibility of polyamide 6 and poly(vinyl acetate) with different degrees of hydrolysis: an atomistic and mesoscopic approach. Macromolecules. 2001;34:5306–16.
35. Vetter T, Mazzotti M, Bronzio J. Slowing the growth rate of ibuprofen crystals using the polymeric additive Pluronic F127. Cryst Growth Des. 2011;11:3813–21.
36. Ewald PP. Die Berechnung optischer und elektrostatischer Gitterpotentiale (evaluation of optical and electrostatic lattice potentials). Ann Phys. 1921;64:253–87.
37. Berendsen HJC, Postma JPM, van Gunsteren WF, DiNola A, Haak JR. Molecular dynamics with coupling to an external bath. J Chem Phys. 1984;81:3684–90.

38. \Andersen HC. Molecular dynamics simulations at constant pressure and/or temperature. J Chem Phys. 1980;72:2384–93.
39. BASF (2012) Technical bulletin. Pluronics® F127 block copolymer surfactant. Available from: http://worldaccount.basf.com/wa/NAFTA/Catalog/ChemicalsNAFTA/doc4/BASF/PRD/30089187. Accessed 16 August 2012.
40. Hofmann D, Fritz L, Ulbrich J, Paul UD. Molecular simulation of small molecule diffusion and solution in dense amorphous polysiloxanes and polyimides. Comput Theor Polym Sci. 2000;10:419–36.
41. Theodorou DN, Suter UW. Detailed molecular structure of a vinyl polymer glass. Macromolecules. 1985;18:1467–78.
42. Einstein A. Von der molekulärkinetischen Theorie der Wärme gefordete Bewegung von in ruhenden Flüssigkeiten suspendierten Teilchen (The motion of elements suspended in static liquids as claimed in the molecular kinetic theory of heat). Ann Phys. 1905;17:549–60.
43. Liebenberg W, Engelbrecht E, Wessels A, Devarakonda B, Yang W, de Villiers MM. A comparative study of the release of active ingredients from semi-solid cosmeceuticals measured with a Franz, enhancer or flow-through cell diffusion apparatus. J Food Drug Anal (Yaowu Shipin Fenxi). 2004;12:19–28.
44. Tanaka K. Self-diffusion coefficients of water in pure water and in aqueous solutions of several electrolytes with ^{18}O and ^{2}H as tracers. J Chem Soc Faraday Trans 1 Phys Chem Condensed Phases. 1978;74:1879–81.
45. Arrhenius S. On the reaction velocity of the inversion of cane sugar by acids. Z Phys Chem. 1889;4:226.